

Orbital coupling and superconductivity in the iron pnictides

Junhua Zhang,¹ Rastko Sknepnek,¹ Rafael M. Fernandes,¹ and Jörg Schmalian¹

¹*Department of Physics and Astronomy and Ames Laboratory, Iowa State University, Ames, Iowa 50011, USA*

(Dated: March 22, 2022)

We demonstrate that strong inter-orbital interaction is very efficient to achieve superconductivity due to magnetic fluctuations in the iron pnictides. Fermi surface states that are coupled by the antiferromagnetic wave vector are often of different orbital nature, causing pair-hopping interactions between distinct Fe-3d orbitals to become important. Performing a self-consistent FLEX calculation below T_c we determine the superconducting order parameter as function of intra- and inter-orbital couplings. We find an s^\pm -pairing state with $T_c \simeq 80\text{K}$ for realistic parameters.

High superconducting transition temperatures and the proximity to antiferromagnetic order strongly suggest an electronic pairing mechanism in the FeAs systems[1]. The vicinity to a spin density wave instability with paramagnons as dominant collective mode is key for spin fluctuation induced superconductivity, where pairing is the result of paramagnon exchange. However, superconductivity in the iron pnictides occurs not only in the immediate vicinity of the magnetically ordered state and the viability of spin fluctuation induced pairing becomes an issue that requires a quantitative analysis. In addition, multi-orbital effects of the Fe-3d bands with a filling of approximately six electrons per Fe-site add to the complexity of these systems: Electronic structure calculations[2, 3] yield two sets of Fermi surface sheets, one around the center of the Brillouin zone (Γ -point) and the other around the M -point, shifted from Γ by the magnetic ordering vector \mathbf{Q} [4]. Inter-band scattering of electrons has been proposed to lead to unconventional pairing[3, 5, 6, 7, 8, 9, 10, 11, 12, 13]. While for certain parameters other solutions exist[9, 10, 13], inter-band coupling tends to support the s^\pm -pairing state where the gap functions on the two Fermi surface sheets have opposite sign.

Crucial for all scenarios based upon inter-band scattering is that states $|\psi_{\Gamma,\mathbf{k}}\rangle$ on one Fermi surface are coupled to states $|\psi_{M,\mathbf{k}+\mathbf{Q}}\rangle$ on another Fermi surface, and vice versa. The natural starting point to describe electron-electron interactions in transition metals is however not in terms of bands, but rather in terms of local orbitals $|a\rangle$. Here $a = xz, yz, xy, x^2 - y^2$ and $3z^2 - r^2$ refers to the Fe-3d orbitals, with intra- and inter-orbital direct Coulomb interactions, U and U' , as well as Hund's rule coupling J_H and inter-orbital pair hopping J' . The importance of orbital effects in the iron pnictides was also stressed in Ref.[14]. As we will see below, the dominant effective spin-fluctuation induced pairing interaction in a multi-orbital system is of the pair-hopping form:

$$H_{\text{pair}} = \sum_{\mathbf{k}, \mathbf{k}'; a, b} W_{\mathbf{k}, \mathbf{k}'}^{ab} d_{\mathbf{k}\mathbf{a}\uparrow}^\dagger d_{-\mathbf{k}\mathbf{a}\downarrow}^\dagger d_{-\mathbf{k}'\mathbf{b}\downarrow} d_{\mathbf{k}'\mathbf{b}\uparrow}. \quad (1)$$

A pair of electrons in orbital b is scattered into a pair in orbital a . For $a = b$ we consider intra-orbital pair-

ing interactions, while $a \neq b$ corresponds to an inter-orbital pairing interaction. In both cases, Cooper pairs are predominantly made up of electrons in the same orbital: $\langle d_{-\mathbf{k}\mathbf{a}\downarrow} d_{\mathbf{k}\mathbf{a}\uparrow} \rangle \neq 0$. In the band picture this yields the inter-band pairing interaction

$$W_{\mathbf{k}, \mathbf{k}'}^{\Gamma, M} \simeq \sum_{ab} \langle \psi_{\Gamma, \mathbf{k}} | a \rangle^2 W_{\mathbf{k}, \mathbf{k}'}^{ab} \langle b | \psi_{M, \mathbf{k}'} \rangle^2. \quad (2)$$

The dominant momentum transfer in the spin fluctuation approach is of course $\mathbf{k} - \mathbf{k}' = \mathbf{Q}$. It is interesting to observe that electronic structure calculations show that $|\psi_{\Gamma, \mathbf{k}}\rangle$ and $|\psi_{M, \mathbf{k}+\mathbf{Q}}\rangle$ are often dominated by *different* orbitals. For example, if $\langle xz | \psi_{\Gamma, \mathbf{k}} \rangle$ is large, it holds that $\langle xz | \psi_{M, \mathbf{k}+\mathbf{Q}} \rangle$ for the same \mathbf{k} is small, while $\langle xy | \psi_{M, \mathbf{k}+\mathbf{Q}} \rangle$ might be large. In Fig. 1a we illustrate this effect where distinct colors refer to the dominant orbitals on the Fermi surface. We used the tight binding parametrization of the five band model of Ref.[13], where a similar plot was presented. The three dominant orbitals on the Fermi surface are xz, yz , and xy . Connecting a Fermi surface point by $\mathbf{Q} = (\pi, 0)$ or $(0, \pi)$ leads in most cases to a different orbital. Thus, the orbital composition of the wave function at the Fermi surface *frustrates* intra-orbital pairing. In other words, inter-band but intra-orbital scattering of spin fluctuations ($\propto W_{\mathbf{k}, \mathbf{k}'}^{aa}$) provides a less efficient pairing glue, if compared to inter-orbital scattering $\propto W_{\mathbf{k}, \mathbf{k}'}^{ab}$ ($a \neq b$) of equal size. It is crucial to determine under what conditions collective paramagnons with strong inter-orbital pair-hopping exist.

In this Rapid Communication we solve the two-orbital many-body problem in the superconducting state for varying intra-orbital (U) and inter-orbital (U' , $J \equiv J_H = J'$) couplings within the self-consistent fluctuation exchange (FLEX) approximation[15]. We obtain superconductivity with s^\pm -pairing. The superconducting order parameter is determined self-consistently and vanishes at $T_c \simeq 80\text{K}$. We demonstrate that strong collective inter-orbital spin-fluctuations are efficient to increase superconductivity. To solve the FLEX equation on the imaginary frequency axis for a lattice of $N = 32 \times 32$ sites and at temperatures as low as $T \simeq 10\text{K}$ we require $2^{13} = 8192$ Matsubara frequencies. At the moment, this restricts our analysis to consider only two orbitals. In Fig. 1b we show

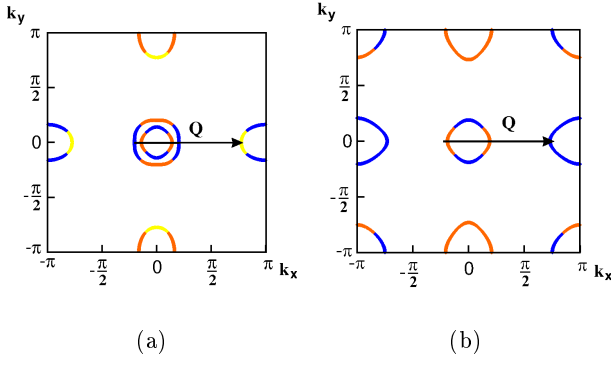


Figure 1: (Color online) Fermi surface of the five-orbital (a) and two-orbital (b) tight binding model of the Fe-3d states in the unfolded Brillouin zone (one iron atom per unit cell). Colors indicate the dominant orbital that contributes to the bands: xz (orange/gray), yz (blue/dark gray), and xy (yellow/light gray). The antiferromagnetic vector $\mathbf{Q} = (\pi, 0)$ mostly connects states dominated by *different* orbitals. The tight binding parameters are from Ref.[13] for panel (a) and Ref.[12] for panel (b).

the Fermi surface of a two band model with d_{xz} and d_{yz} orbitals. The mentioned frustration of intra-orbital pairing is less pronounced for this simplified model. Yet, the phase space for inter-orbital pairing interactions is still larger compared to intra-orbital interactions.

The model: We consider the Hamiltonian

$$H = \sum_{\mathbf{k}, ab, \sigma} \varepsilon_{\mathbf{k}}^{ab} d_{\mathbf{k}a\sigma}^\dagger d_{\mathbf{k}b\sigma} - J_H \sum_{i, a > b} \left(2\mathbf{s}_{ia} \cdot \mathbf{s}_{ib} + \frac{1}{2} n_{ia} n_{ib} \right) + U \sum_{i, a} n_{ia\uparrow} n_{ia\downarrow} + U' \sum_{i, a > b} n_{ia} n_{ib} + J' \sum_{i, a \neq b} b_{ia}^\dagger b_{ib}, \quad (3)$$

where $n_{ia\sigma} = d_{ia\sigma}^\dagger d_{ia\sigma}$ is the occupation of the orbital a with spin σ at site i and $n_{ia} = \sum_{\sigma} n_{ia\sigma}$. $\mathbf{s}_{ia} = \frac{1}{2} \sum_{\sigma\sigma'} d_{ia\sigma}^\dagger \boldsymbol{\sigma} \sigma' d_{ia\sigma'}$ is the electron spin and $b_{ia}^\dagger = d_{ia\uparrow}^\dagger d_{ia\downarrow}^\dagger$ the pair creation operator, respectively. For the tight binding band structure we use $\varepsilon_{\mathbf{k}}^{xy} = \varepsilon_{\mathbf{k}}^{yx} = -4t_4 \sin k_x \sin k_y$ and $\varepsilon_{\mathbf{k}}^{aa} = -2t_1 \cos k_a - 2t_2 \cos k_{\bar{a}} - 4t_3 \cos k_x \cos k_y - \mu$, where $a = x$ (y) stands for xz (yz) orbital as well as the momentum coordinate with $\bar{x} = y$ and $\bar{y} = x$. We use $t_1 = -0.33$ eV, $t_2 = 0.385$ eV, $t_3 = -0.234$ eV, and $t_4 = -0.26$ eV of Ref. [12]. Our results were obtained for a filling of $n = 1.88$ electrons per site, corresponding to moderate hole doping. The filling of a subset of bands is primarily determined to reproduce realistic Fermi surface geometries and yields commensurate magnetic fluctuations.

The multi-orbital fluctuation exchange approach: The FLEX equations for a multi-orbital problem are given in Ref.[16]. In the normal state one obtains the single particle self energy Σ_k^{ab} which yields the single particle propagator G_k^{ab} . Here $k = (\mathbf{k}, i\omega_n)$ stands for the momentum vector \mathbf{k} and the Matsubara frequency $\omega_n = (2n + 1)\pi T$ with temperature T . As it is important for our subse-

quent discussion we summarize the key equations that occur in the superconducting state and determine the anomalous self energy:

$$\Phi_k^{ab} = \sum_{k'} \sum_{cd} \Gamma_{k-k'}^{ac, db} F_{k'}^{cd}. \quad (4)$$

This equation is the strong coupling version of the gap-equation. $\sum_k \dots = \frac{T}{N} \sum_{\mathbf{k}, n} \dots$ stands for the summation over momenta and Matsubara frequencies. F_k^{ab} is the anomalous Green's function, that determines the Cooper pair expectation value $\langle d_{\mathbf{k}a\uparrow} d_{-\mathbf{k}b\downarrow} \rangle = T \sum_n F_k^{ab}$. Furthermore, $\Gamma_q^{ac, db}$ is the dynamic pairing interaction that depends on momentum, frequency and the orbital states involved, where $q = (\mathbf{q}, i\nu_n)$ with $\nu_n = 2n\pi T$. Introducing the two-particle quantum numbers $A = (a, c)$ and $B = (d, b)$ that label the rows and columns of two-particle states, the interaction, $\Gamma_q^{A, B} = \Gamma_q^{ac, db}$ becomes a $m^2 \times m^2$ -dimensional symmetric operator $\hat{\Gamma}_q$, where m is the number of orbitals. It is now straightforward to sum particle hole ladder and bubble diagrams. It follows:

$$\hat{\Gamma}_q = \frac{3}{2} \hat{V}_{s, q} + \frac{1}{2} \hat{V}_{c, q} + \hat{V}_{HF}, \quad (5)$$

where interactions in the spin and charge channel are:

$$\hat{V}_{s(c), q} = \pm \hat{U}_{s(c)} \left(1 \mp \hat{\chi}_{s(c), q} \hat{U}_{s(c)} \right)^{-1} \hat{\chi}_{s(c), q} \hat{U}_{s(c)} - \frac{1}{4} \hat{U}_{s(c)} (\hat{\chi}_{s, q} - \hat{\chi}_{c, q}) \hat{U}_{s(c)}. \quad (6)$$

\hat{U}_s and \hat{U}_c are also $m^2 \times m^2$ -dimensional matrices of the interaction in the spin and charge channel, respectively. Close to a magnetic instability, the dominant contribution to $\hat{\Gamma}_q$ comes from the spin channel $\hat{V}_{s, q}$ due to the Stoner enhancement $\left(1 - \hat{\chi}_{s, q} \hat{U}_s \right)^{-1}$. For the interaction matrix in the spin sector holds $U_s^{aa, aa} = U$, while for $a \neq b$ holds $U_s^{ab, ab} = U'$, $U_s^{ab, ba} = J'$ and $U_s^{aa, bb} = J_H$. The Hartree-Fock contribution $\hat{V}_{HF} = (\hat{U}_s + \hat{U}_c)/2$ is suppressing superconductivity, an effect caused by the repulsive direct Coulomb interaction. We find that the impact of direct Coulomb interaction is strongly reduced in the s^\pm state with small, but finite, average $\langle d_{ia\uparrow} d_{ia\downarrow} \rangle$ for local Cooper pairing. For a discussion of this Coulomb avoidance see Ref. [17]. Finally, the irreducible particle hole bubble $\hat{\chi}_{s(c), q}$ is determined by normal and anomalous Green's functions: $\chi_{s(c), q}^{ab, cd} = -\sum_k \left(G_{k+q}^{ac} G_k^{db} \pm F_{k+q}^{ad} F_k^{cb*} \right)$, assuming time reversal invariance and singlet pairing. We solved the set of coupled FLEX equations self consistently in the superconducting state.

The pairing state and its T-dependence: The momentum dependence of the anomalous self energy Φ_k^{aa} is shown in the insets of Figs. 3 and 4. The symmetry of Φ_k^{ab} and of the Hamiltonian are the same, corresponding to s -wave pairing[12]. Nevertheless, the sign of Φ_k^{aa} is

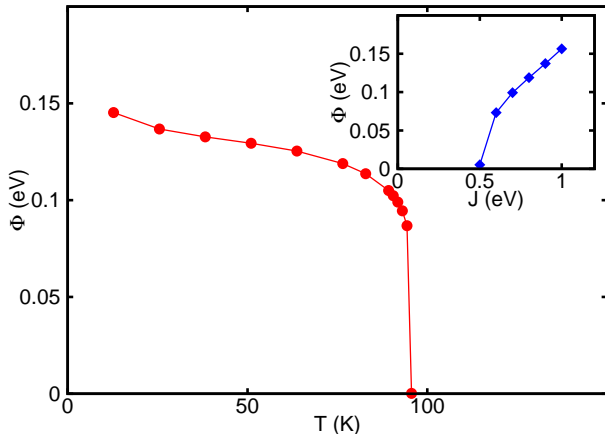


Figure 2: (Color online) Temperature dependence of the anomalous self energy $\Phi_{\mathbf{k}=0,\pi T}^{xx}$, proportional to the superconducting order parameter, for $U = 1.5\text{eV}$, $U' = 1.2\text{eV}$, and $J = 0.8\text{eV}$. The inset shows the increase of $\Phi_{\mathbf{k}}^{xx}$ with increasing inter-orbital coupling J at $T = 60\text{K}$.

opposite on Fermi surface sheets around Γ and M , i.e., we obtain the s^{\pm} pairing state that was proposed in Ref. [3]. While in general such a state can have nodes of the gap on the Fermi surface, our solution corresponds to a fully gapped state. For a recent discussion of the s^{\pm} -state see Ref. [17]. In Fig. 2 we show the temperature dependence of the anomalous self energy $\Phi_{\mathbf{k}=0}^{xx}$, which is proportional to the superconducting order parameter. The feedback of the opening of a pairing gap onto the dynamic pairing interaction leads to the rather rapid growth of the order parameter below T_c [18]. $T_c \simeq 80\text{K}$ is indeed of the correct order of magnitude. In the normal state the dynamics of paramagnons is overdamped $\Gamma_{\mathbf{Q},\omega}^{aa,aa} \sim (1 + |\omega|/\omega_s)^{-1}$. For the parameters of Fig. 2 we find $\omega_s(T_c) = 37\text{meV}$. This energy scale is reduced compared to the typical electronic energies because of the Stoner enhancement. It sets the scale for the Lorentzian lineshape of inelastic neutron scattering at \mathbf{Q} above T_c . A strong pairing interaction is caused by a significant Stoner enhancement, which is controlled by the value of the magnetic inter-orbital coupling, J . This is demonstrated in the inset of Fig. 2 where we show the sensitivity of superconducting order with respect to J at $T = 60\text{K}$.

Intra- versus inter-orbital pairing: For the pnictides, the pairing vertex $\widehat{\Gamma}_{\mathbf{q}}$ in Eq. (4) is dominated by a few matrix elements. We find that $\chi_{s,\mathbf{q}}^{A,B}$ at $\mathbf{q} \simeq \mathbf{Q}$ has comparable diagonal elements χ_d and somewhat smaller counter diagonal elements $\chi_{\bar{d}}$ in two-particle space, while all other matrix elements are negligible. It then follows from Eq. (6) that the dominant matrix elements of $\widehat{\Gamma}_{\mathbf{q}}$ are $\Gamma_q^{ab,ba}$. If one interprets $\Gamma_q^{ab,ba}$ as effective low energy interaction, the combination of orbital indices yields precisely the pair-hopping form Eq. (1) with $W_{\mathbf{k},\mathbf{k}'}^{ab} = \Gamma_{\mathbf{k}-\mathbf{k}'}^{ab,ba}$. The effective Stoner enhancements for same orbitals $a = b$ are $\Gamma_q^{aa,aa} \simeq$

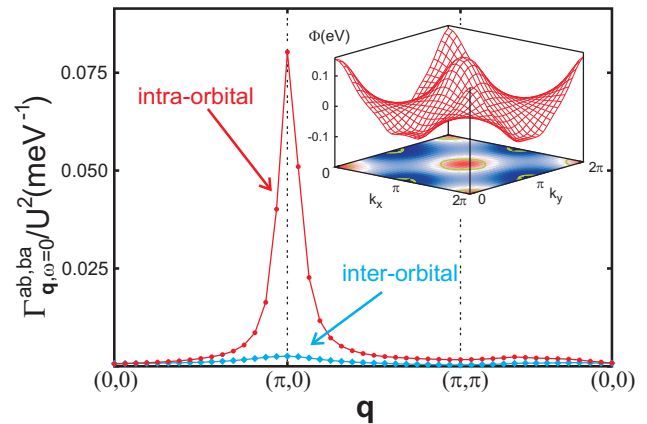


Figure 3: (Color online) Intra-orbital and inter-orbital pairing interaction at zero frequency as function of momentum for $U = 1.5\text{eV}$, $U' = 1\text{eV}$ and $J = 1\text{eV}$ at a temperature of $T = 70\text{K}$ along with the self-consistently determined anomalous self energy $\Phi_{\mathbf{k},\pi T}^{xx}$ (inset) that determines the sign and momentum dependence of the superconducting gap. The pairing interaction is peaked for momenta $\mathbf{Q} = (\pi, 0)$ and $(0, \pi)$. The anomalous self energy corresponds to s^{\pm} -pairing with opposite sign of the gap on Fermi surface sheets around Γ and M . Inter-orbital pairing is significantly smaller.

$(U + J_H)(1 - (U + J_H)(\chi_d + \chi_{\bar{d}}))^{-1}$ while for $a \neq b$ follows $\Gamma_q^{ab,ba} \simeq (U' + J')(1 - (U' + J')(\chi_d + \chi_{\bar{d}}))^{-1}$. Whenever U is significantly larger than the other couplings, Eq. (4) is dominated by interactions within the same orbital. As mentioned, the intra-orbital pairing interaction is however rather inefficient. The situation changes when we consider comparable values for the intra- and inter-orbital Coulomb enhancements: $U + J_H \gtrsim U' + J'$, i.e. a regime with strong orbital fluctuations. The pairing interaction is enhanced, as the nature of the wave functions on the Fermi surface can efficiently take advantage of coupling between distinct orbitals, see Eq. (2) and Fig.1.

The condition $U + J_H \gtrsim U' + J'$ is at variance with the relations $U = U' + 2J$ and $J' = J_H$ that result from the rotational symmetry of the bare Coulomb interaction[19], if combined with evidence for sizable Hund coupling[20, 21]. We stress however that the interaction parameters that enter an approximate theory such as FLEX are not identical to the bare Coulomb matrix elements[22]. FLEX ignores crucial vertex corrections and U , U' and J should rather be considered low energy interaction parameters that have been renormalized by high energy excitations. Performing a renormalization of the Coulomb interactions within a multiband version of the Kanamori scattering matrix approach[23], we indeed find that $U + J_H \simeq U' + J'$ for realistic values of the bare Coulomb matrix elements of Fe[24]. In this approach, particle-particle excitations couple states with \mathbf{k} and $-\mathbf{k}$, i.e., states of same orbital nature. This reduces U more strongly than U' , J_H , and J' . Thus, constraints due to

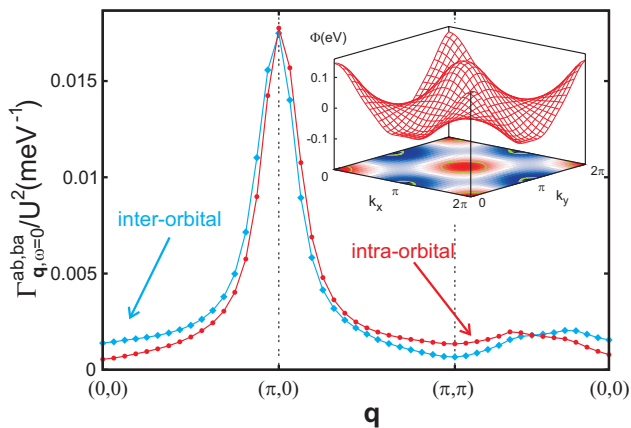


Figure 4: (Color online) Same as Fig. 3 but for parameters $U = U' = 1.5\text{eV}$ and $J = 1\text{eV}$ with same temperature $T = 70\text{K}$. Now intra- and inter-orbital couplings are of comparable size, leading to the same superconducting order parameter as for Fig. 3, however for much smaller pairing strength, associated with moderate antiferromagnetic fluctuations (see the different scale compared to Fig. 3).

rotational invariance do not apply for low energy vertices that enter FLEX, and intra-orbital and inter-orbital pairing interactions can easily be comparable. The underlying low density expansion makes the Kanamori scattering matrix renormalization a very sensible approach for the pnictides, given their near semimetallic electronic structure.

In Figs. 3 and 4 we compare two different parameter sets that yield almost the same value for Φ_k^{aa} at the same temperature. The first case has a predominant intra-orbital interaction which needs to be very large in order to achieve pairing. In the other case the same pairing amplitude is obtained from intra- and inter-orbital pairing interactions. $\Gamma_q^{ab,ba}$ in Fig. 4 are almost one fifth of the pure intra-band interaction in Fig. 3, demonstrating the efficient role played by inter-orbital magnetic pairing interactions in the iron pnictides.

In summary we presented a self-consistent FLEX analysis of a two orbital model of the FeAs systems in the superconducting state. We determined the temperature dependence of the superconducting order parameter and showed that $T_c \simeq 60 - 80\text{K}$, of the order of the experimental values, are clearly possible. The pairing state is s^\pm with opposite sign of the gap on Fermi surface sheets around Γ and M [3]. In the iron pnictides, states that are coupled by the antiferromagnetic wave vector are often dominated by different local Fe-3d orbitals. This makes a purely intra-orbital pairing interaction quite inefficient. Inter-orbital pairing due to antiferromagnetic fluctuations yields the same pairing amplitude for much smaller Stoner enhancement, i.e., for more moderate values of the magnetic correlation length. We expect this effect to be even stronger in a more realistic five-orbital description of the iron pnictides. Collective low energy

pairing interaction between like and unlike orbitals, i.e., strong orbital fluctuations, significantly enhances the viability of the spin fluctuation approach for superconductivity in the pnictides.

We are grateful to A. V. Chubukov and I. I. Mazin for helpful discussions. This research was supported by the Ames Laboratory, operated for the U.S. Department of Energy by Iowa State University under Contract No. DE-AC02-07CH11358.

- [1] Y. Kamihara, T. Watanabe, M. Hirano, and H. Hosono, *J. Am. Chem. Soc.* **130**, 3296 (2008).
- [2] D. J. Singh and M.-H. Du, *Phys. Rev. Lett.* **100**, 237003 (2008).
- [3] I.I. Mazin, D.J. Singh, M.D. Johannes, M.H. Du, *Phys. Rev. Lett.* **101**, 057003 (2008).
- [4] C. de la Cruz, Q. Huang, J. W. Lynn, J. Li, W. Ratcliff II, J. L. Zarestky, H. A. Mook, G. F. Chen, J. L. Luo, N. L. Wang, P. Dai, *Nature* **453**, 899 (2008).
- [5] K. Kuroki, S. Onari, R. Arita, H. Usui, Y. Tanaka, H. Kontani, H. Aoki, *Phys. Rev. Lett.* **101**, 087004 (2008).
- [6] A.V. Chubukov, D. V. Efremov, I. Eremin, *Phys. Rev. B* **78**, 134512 (2008).
- [7] V. Cvetković, Z. Tešanović, *Euro. Phys. Lett.* **85**, 37002 (2009).
- [8] H. Ikeda, *J. Phys. Soc. Jpn.* **77**, 123707 (2008).
- [9] K. Seo, B. A. Bernevig, and J. Hu, *Phys. Rev. Lett.* **101**, 206404 (2008).
- [10] Z.-J. Yao, J.-X. Li, Z. D. Wang, *New J. Phys.* **11**, 025009 (2009).
- [11] F. Wang, H. Zhai, Y. Ran, A. Vishwanath, D.-H. Lee, *Phys. Rev. Lett.* **102**, 047005 (2009).
- [12] R. Sknepnek, G. Samolyuk, Y.-B. Lee, J. Schmalian, *Phys. Rev. B* **79**, 054511(2009).
- [13] S. Graser, T. A. Maier, P. J. Hirschfeld, D. J. Scalapino, *New J. Phys.* **11**, 025016 (2009).
- [14] T. D. Stanescu, V. Galitski, S. Das Sarma, *Phys. Rev. B* **78**, 195114 (2008).
- [15] N. E. Bickers, D. J. Scalapino, and S. R. White, *Phys. Rev. Lett.* **62**, 961 (1989).
- [16] T. Takimoto, T. Hotta, and K. Ueda, *Phys. Rev. B*, **69**, 104504 (2004).
- [17] I.I. Mazin, and J. Schmalian, to appear in *Physica C* (2009); arXiv:0901.4790.
- [18] P. Monthoux and D. J. Scalapino, *Phys. Rev. Lett.* **72**, 1874 (1994).
- [19] C. Castellani, C. R. Natoli, and J. Ranninger, *Phys. Rev. B* **18**, 4945 (1978).
- [20] T. Kroll, S. Bonhommeau, T. Kachel, H. A. Durr, J. Werner, G. Behr, A. Koitzsch, R. Hubel, S. Leger, R. Schonfelder, A. K. Ariffin, R. Manzke, F. M. F. de Groot, J. Fink, H. Eschrig, B. Buchner, and M. Knupfer, *Phys. Rev. B* **78**, 220502(R) (2008).
- [21] K. Haule, G. Kotliar, *New J. Phys.* **11**, 025021 (2009).
- [22] L. Chen, C. Bourbonnais, T. Li, A.-M. S. Tremblay, *Phys. Rev. Lett.* **66**, 369 (1991); N. Bulut, D. J. Scalapino and S. R. White, *Phys. Rev. B* **47**, 2742 (1993).
- [23] J. Kanamori *Progr. of Theoret. Phys.* **30**, 275 (1963).
- [24] T. Miyake and F. Aryasetiawan, *Phys. Rev. B* **77**, 085122 (2008).